
Figures and figure supplements

Dynamics of pulsatile activities of arcuate kisspeptin neurons in aging female mice

Teppei Goto et al.

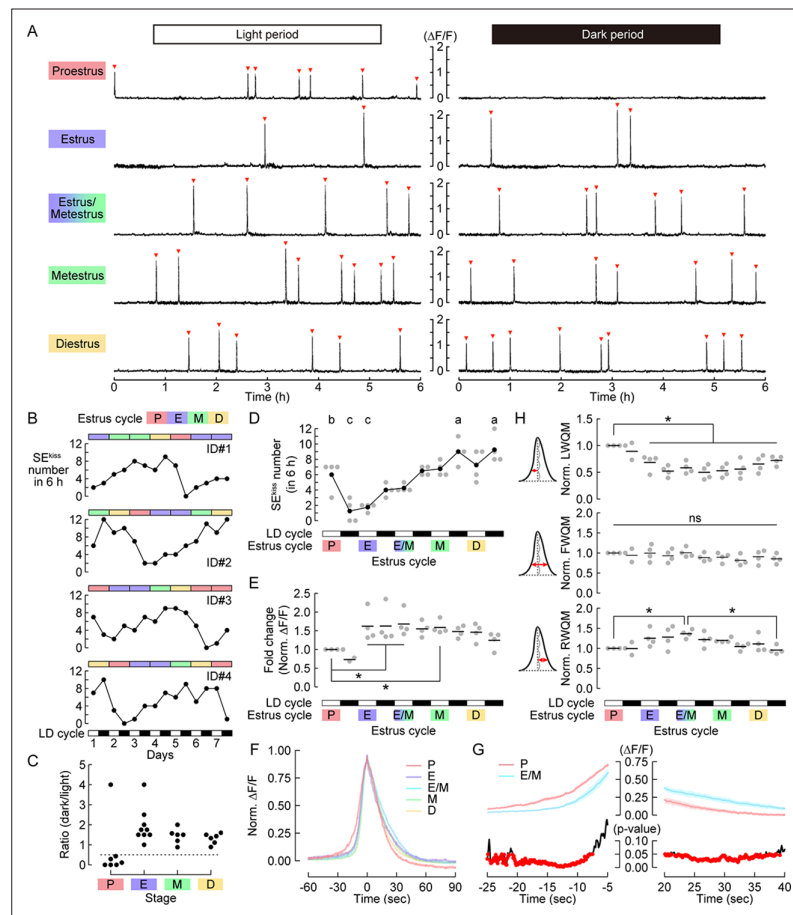


Figure 1. Dynamics of synchronous episodes of ARC^{kiss} (SEs^{kiss}) in the regular estrus cycle of the reproductive phase. **(A)** Representative 6 h photometry raw data of SEs^{kiss} in each stage of the estrus cycle. Red arrowheads indicate SEs^{kiss}. **(B)** Numbers of SEs^{kiss} (lower: line plots) along with the estrus cycle stages (upper: color bars) for 7 days (n=4 animals). SEs^{kiss} were recorded for 6 h in both light and dark (LD) periods. **(C)** The ratio of SEs^{kiss} in each dark period normalized to those in the preceding light period. Dotted line = 0.5. **(D)** Numbers of SEs^{kiss} per 6 h in 5 days along with the estrus cycle anchoring at proestrus as Day 0. Different letters (a–c) in the upper part of the graph denote significant differences at p<0.05 by one-way repeated measures ANOVA followed by the Tukey–Kramer post hoc test. **(E)** Intensities of SEs^{kiss} as measured by the $\Delta F/F$ values in each estrus stage normalized to that in the light period of the proestrus. *p<0.05 by one-way repeated measures ANOVA followed by the Tukey–Kramer post hoc test. **(F)** Averaged traces of SEs^{kiss} waveforms in the light period of each estrus stage. **(G)** Top, averaged traces magnifying the onset and offset of SEs^{kiss} in the proestrus and estrus/metestrus stages in the light period. Data are expressed as mean \pm SEM. Bottom, p-value by t-test. Red dots represent p-values <0.05. **(H)** Quantifications of detailed parameters of SEs^{kiss} waveforms in each estrus stage: the normalized LWQM, FWQM, and RWQM. *p<0.05 by one-way repeated measures ANOVA followed by the Tukey–Kramer post hoc test. P: proestrus, E: estrus, M: metestrus, D: diestrus.

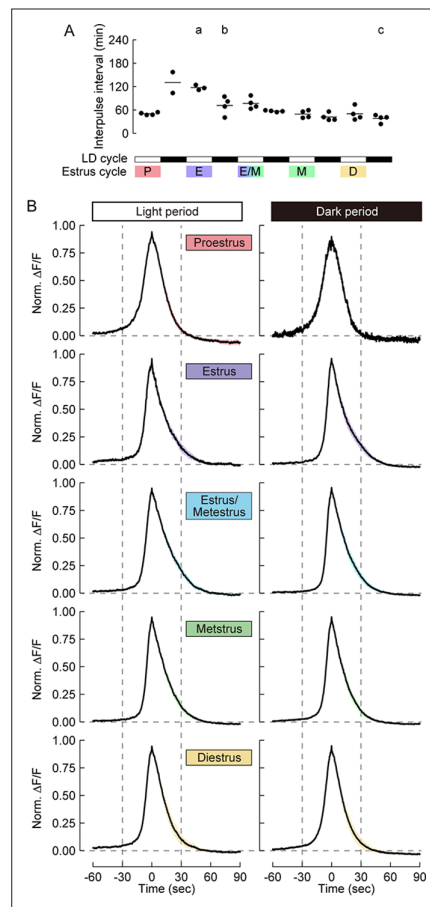


Figure 1—figure supplement 1. Inter-pulse intervals and waveforms of synchronous episodes of ARC^{kiss} (SEs^{kiss}) in each estrus stage. **(A)** Inter-pulse intervals of SEs^{kiss} in each estrus stage. Different letters (a–c) in the upper part of the graph denote significant differences at $p < 0.05$ by one-way repeated measures ANOVA followed by the Tukey–Kramer post hoc test. **(B)** SE^{kiss} waveforms in the light and dark periods of each estrus stage. Data are expressed as mean (black line) \pm SEM (colored shadow).

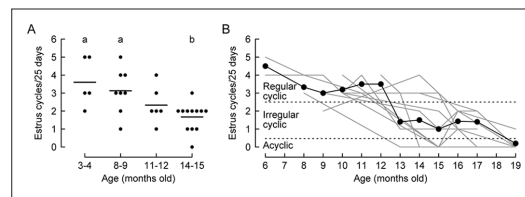


Figure 2. Decrease in estrus cycle frequency during the transition to reproductive senescence. **(A)** Number of estrus cycles per 25 days at 3–4 ($n=5$), 8–9 ($n=8$), 11–12 ($n=6$), and 14–15 ($n=12$) months in old wild-type C57BL/6 mice. Different letters (a, b) in the upper part of the graph denote significant differences at $p<0.05$ by one-way ANOVA followed by the Tukey–Kramer post hoc test. **(B)** Chronic monitoring of estrus cycle frequency from the individuals used for Ca^{2+} imaging of synchronous episodes of ARC^{kiss} (SEs^{kiss}) (C57BL/6 Kiss-Cre mice with AAV-mediated GCaMP6s expression). Black: average number of estrus cycles, gray: individual data ($n=12$ animals in total).

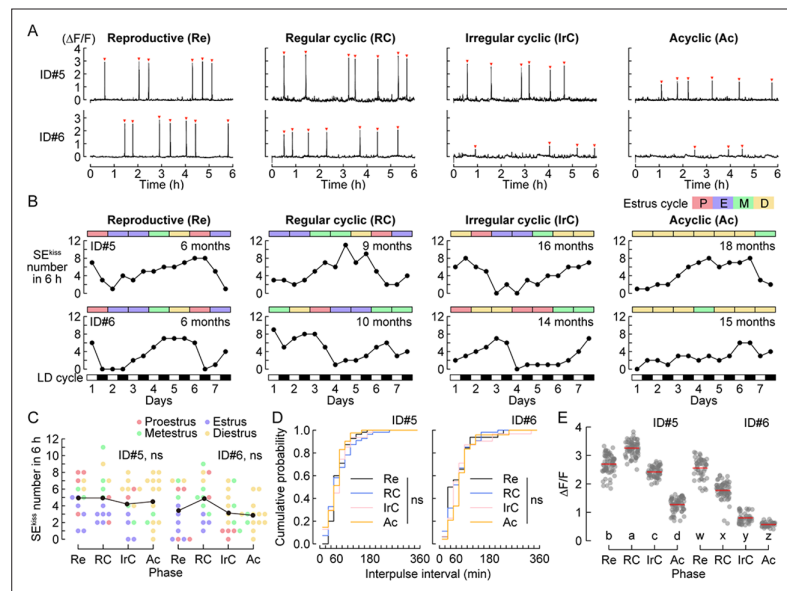


Figure 3. Chronic monitoring of synchronous episodes of ARC^{kiss} (SEs^{kiss}) from the reproductive to acyclic phase. (A) Representative photometry raw data of SEs^{kiss} in the diestrus stage from the reproductive to acyclic phase (n=2 animals). Red arrowheads indicate SEs^{kiss}. (B) Numbers of SEs^{kiss} in the estrus stages (color bars) for 7 days from the reproductive to acyclic phase. SEs^{kiss} were recorded for 6 h in both light and dark periods. (C) Number of SEs^{kiss} in individual estrus stages (shown in different colors) of individual female mice. ns: not significant by one-way ANOVA. (D) Cumulative probability of inter-pulse interval. ns: not significant by the Kolmogorov–Smirnov test. (E) Peak height as assessed by ΔF/F of SEs^{kiss} from the reproductive to acyclic phase. Different letters (a–d, w–z) in the lower part of the graph denote significant differences at p<0.05 by the Kruskal–Wallis test followed by the Mann–Whitney U test. Re; reproductive, RC; regular cyclic, IrC; irregular cyclic, Ac; acyclic.

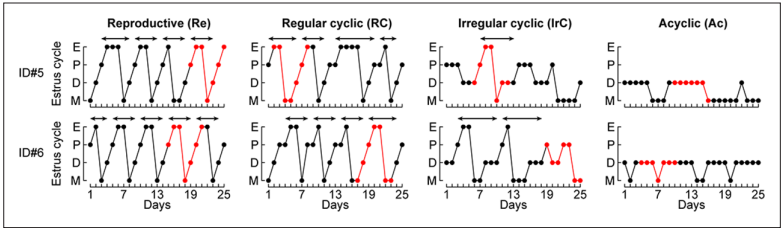


Figure 3—figure supplement 1. Raw data of the estrus cycle, related to **Figure 3**. Graphical representation of estrus stage within a 25 day time window from the reproductive to acyclic phase (n=2 animals). Red dots and lines represent the photometric recording timing shown in **Figure 3B**. Arrows indicate one estrus cycle.

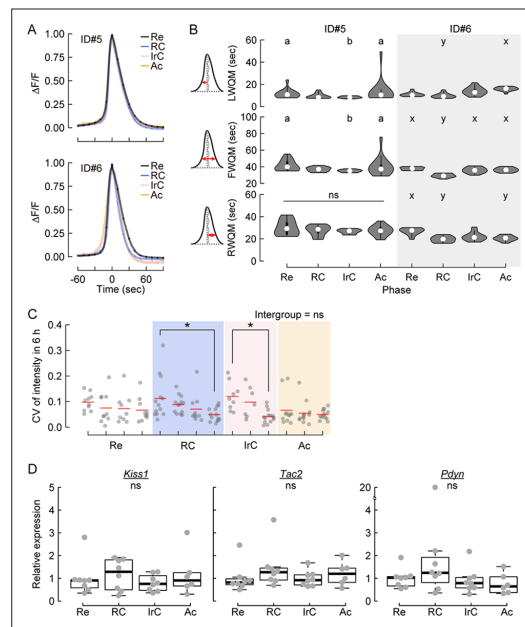


Figure 3—figure supplement 2. Waveforms and intensities of synchronous episodes of ARC^{kiss} (SEs^{kiss}), and gene expression analysis. (A) Averaged traces of SE^{kiss} waveforms of the same female mice in the reproductive (Re), regular cyclic (RC), irregular cyclic (IrC), and acyclic (Ac) phases. (B) Quantifications of detailed parameters of SE^{kiss} waveforms in individual female mice: LWQM, FWQM, and RWQM as defined in Figure 1. Different letters (a–b, x–y) in the upper part of the graph denote significant differences at $p < 0.05$ by the Kruskal–Wallis test followed by the Mann–Whitney U test. In ID#5, the shape of the waveform was changed in the IrC compared with the Re phase, and the shape reverted in the Ac phase. In ID#6, significant differences in the length of LWQM and RWQM were observed between the Re and Ac phases. The origin of these individual differences is unknown, but the bias of estrus cycles in aging female mice might underlay the variations. (C) Coefficient of variances of the intensities of SEs^{kiss} in a 6 h window from Re, RC, IrC, and Ac individual mice. * $p < 0.05$ by the Kruskal–Wallis test followed by the Mann–Whitney U test. (D) The gene expression levels of *Kiss1*, *Tac2*, and *Pdyn* relative to a reference gene were compared among mice in Re, RC, IrC, and Ac phases ($n=8, 8, 8$, and 6 , respectively) during the diestrus stage of the estrous cycle. Each data point was normalized to an average of the corresponding gene expression in Re phase. ns: not significant by the Kruskal–Wallis test.

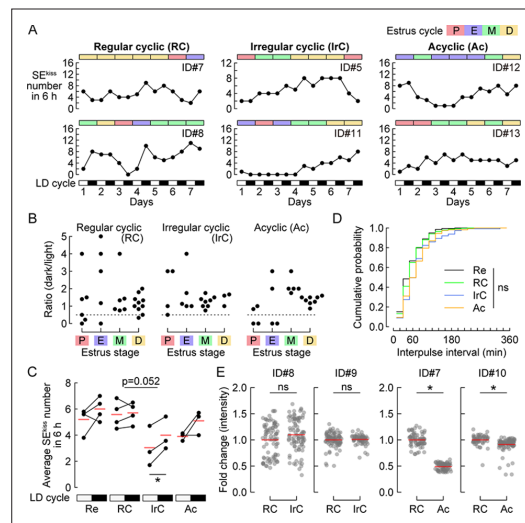


Figure 4. Characterization of synchronous episodes of ARC^{kiss} (SEs^{kiss}) in aging female mice. **(A)** Representative numbers of SEs^{kiss} in the estrus stages (color bars) for 7 days from regular cyclic, irregular cyclic, and acyclic female mice. SEs^{kiss} were recorded for 6 h in both light and dark periods. **(B)** The ratio of SEs^{kiss} in the dark period normalized to those in the preceding light period of regular cyclic (n=4), irregular cyclic (n=3), and acyclic (n=3) female mice, respectively. Dotted line = 0.5. **(C)** Average numbers of SEs^{kiss} in 6 h in the light (open boxes in the LD cycle) and dark (closed boxes in the LD cycle) periods of reproductive (Re), regular cyclic (RC), irregular cyclic (IrC), and acyclic (Ac) mice. Red horizontal lines indicate the mean. No interaction effect between estrus cyclicity and LD cycle was found by two-way ANOVA. * $p < 0.05$ by paired t -test. Of note, the Re group (age 4–6 months) represents a reanalysis of the 5 days of data reported in **Figure 1** (corresponding to one estrus cycle). **(D)** Cumulative probability of inter-peak intervals among the Re (black), RC (green), IrC (blue), and Ac (orange) groups. ns: not significant by the Kolmogorov–Smirnov test. **(E)** Intensities of SEs^{kiss} during reproductive aging as assessed by the fold change of $\Delta F/F$ values in the IrC (#ID8, 9) and Ac (#ID7, 10) phases normalized to those in the RC phase. * $p < 0.05$ by the Mann–Whitney U test. ns: not significant.

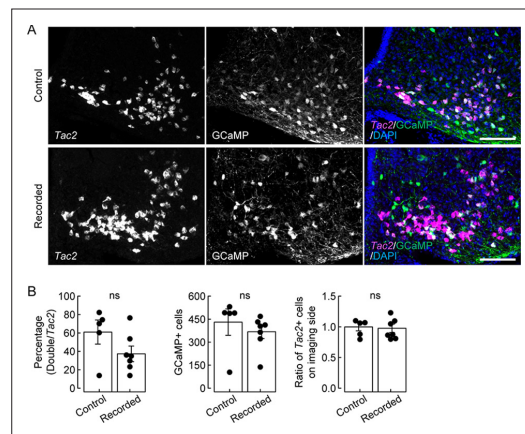


Figure 4—figure supplement 1. Histochemical analysis after imaging. (A) Representative coronal sections of the arcuate nucleus (ARC) showing *Tac2* mRNA expression (magenta), a marker of kisspeptin neurons in the hypothalamic arcuate nucleus (ARC^{kiss}) neurons, and GCaMP6s (green) expression, counterstained with DAPI (blue) in control (healthy reproductive phase without potential damage caused by repeated photometry recording and/or prolonged expression of GCaMP6s, see Methods) and the aging recorded mice. The expressions of *Tac2* mRNA and GCaMP6s protein were well comparable between the reproductive healthy control and aging recorded samples. Scale bars, 100 μm . (B) Left: Quantification of the GCaMP6s targeting efficiency ($Tac2^{+} GCaMP6s^{+}/Tac2^{+}$). Middle: The number of GCaMP6s+ cells. Right: The number of *Tac2*+ cells in the GCaMP6s targeted site normalized to that of the contralateral non-injected and non-imaged site. ns, no significant difference was found between the control and recorded groups by the Mann–Whitney *U* test. $n=5$ and 3 in control and recorded mice, respectively. Error bars, SEM.